Advanced Earth electromagnetism Homework-3

Build an internal geomagnetic using observatory data

Wu Xianshu 12132710

1 Methods and data

According to the Gauss Theory of geomagnetism, we can use the spherical harmonic analysis to describe the earth's main magnetic field. Suppose the magnetic potential of the geomagnetic field obeys Laplace’s equation at the surface of the Earth as well as outside of the Earth, the model can be written as:

$$V(r,\theta,\phi) = a\sum_{n=1}^{N}\sum_{m=0}^{n}\left(g_n^m \cos m\phi + h_n^m \sin m\phi\right)\left(\frac{a}{r}\right)^{n+1} P_n^m(\cos\theta) \tag{1}$$

$$\begin{aligned}
X &= \sum_{n=1}^{N}\sum_{m=0}^{n}\left(\frac{a}{r}\right)^{n+2}\left(g_n^m \cos m\phi + h_n^m \sin m\phi\right)\frac{d}{d\theta}p_n^m(\cos\theta)\\
Y &= \sum_{n=1}^{N}\sum_{m=0}^{n}\frac{-m}{\sin\theta}\left(\frac{a}{r}\right)^{n+2}\left(-g_n^m \sin m\phi + h_n^m \cos m\phi\right)p_m^m(\cos\theta)\\
Z &= \sum_{n=0}^{N}\sum_{m=0}^{n}-(n+1)\left(\frac{a}{r}\right)^{n+2}\left(g_n^m \cos m\phi + h_n^m \sin m\phi\right)p_n^m(\cos\theta)
\end{aligned} \tag{2}$$

The only uncertainty in the formula is g_n^m and h_n^m, which called Gauss Coefficient, and when we have the model and the data, we can get the parameters value by inversion methods. The problem becomes solving the following system of linear algebraic equations (the observations are taken at a spherical surface of the Earth’s mean radius, $r = a$):

$$\mathbf{A}\mathbf{m} = \mathbf{d} \tag{3}$$

$$\mathbf{A} = \begin{bmatrix}
\vdots & \vdots & \vdots & \vdots\\
\cdots & \cos(m\phi_i)\frac{\mathrm{d}P_n^m(\cos\theta_i)}{\mathrm{d}\theta_i} & \sin(m\phi_i)\frac{\mathrm{d}P_n^m(\cos\theta_i)}{\mathrm{d}\theta_i} & \cdots\\
\cdots & m\sin(m\phi_i)\frac{P_n^m(\cos\theta_i)}{\sin\theta_i} & -m\cos(m\phi_i)\frac{P_n^m(\cos\theta_i)}{\sin\theta_i} & \cdots\\
\cdots & -\cos(m\phi_i)P_n^m(\cos\theta_i)(n+1) & -\sin(m\phi_i)P_n^m(\cos\theta_i)(n+1) & \cdots\\
\vdots & \vdots & \vdots & \vdots
\end{bmatrix}; \tag{4}$$

$$\mathbf{m} = \begin{bmatrix} g_1^0\\ \vdots\\ g_n^{n-1}\\ g_n^n\\ h_n^1\\ h_n^2\\ \vdots\\ h_N^N \end{bmatrix};\ \mathbf{d} = \begin{bmatrix} \vdots\\ X_i\\ Y_i\\ Z_i\\ \vdots \end{bmatrix};\ \frac{\mathrm{d}P_n^m(\cos\theta)}{\mathrm{d}\theta} = \frac{\left(n\cos\theta P_n^m - R_n^m P_{n-1}^m\right)}{\sin\theta}; \tag{5}$$

The data in **d** are download from **INTERMAGNET**, the website is https://www.intermagnet.org/data-donnee/download-eng.php. I selected the definitive minute data on 2020-03-05 (Table 1), all available observation stations are included, Figure 1 is a map showing the observatories I used. the 24-hour data of each station are averaged to obtain the observed values of the day, after eliminating the outliers. I wrote a MATLAB script to implement the above process, and built a model up to spherical harmonic degree 4.

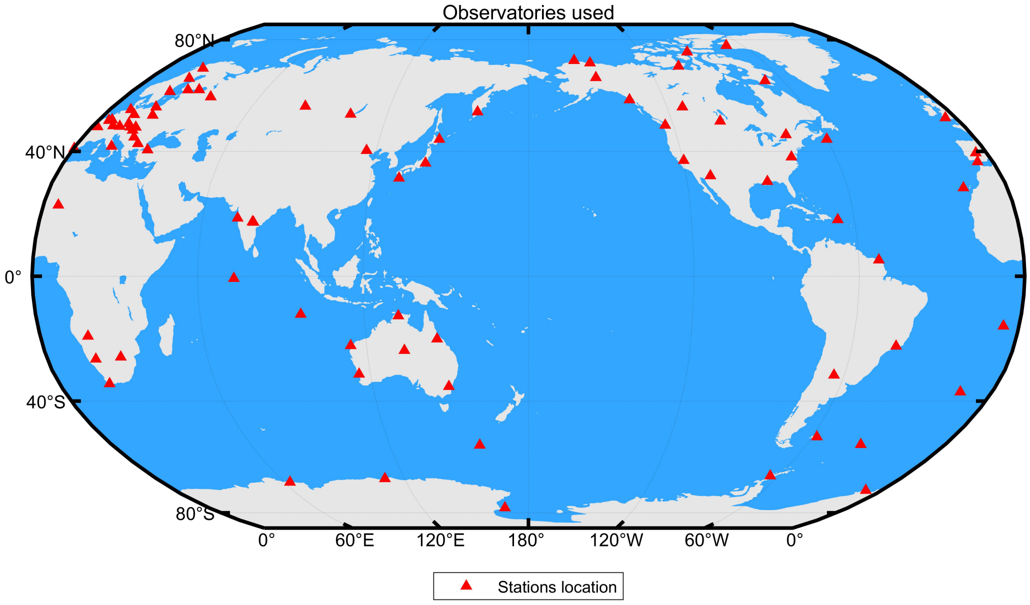

Fig 1. Map showing the observatories I used

Tab 1. A table of data

Index	Name	Latitude	Longitude	X	Y	Z	Date	Index	Name	Latitude	Longitude	X	Y	Z	Date
1	abg	18.62	72.87	38255.32861	290.4123611	20393.29507	20200305	42	kdu	-12.686	132.472	35457.00736	1754.704167	-29582.17056	20200305
2	abk	68.358	18.823	11263.29438	1862.256042	52149.73104	20200305	43	kep	-54.282	323.507	15328.23479	-1902.493542	-22927.075	20200305
3	aia	-65.25	295.73	19743.62451	5529.188194	-31781.59625	20200305	44	kmh	-26.541	18.11	10625.24368	-3290.684375	-24317.20576	20200305
4	asp	-23.761	133.883	30118.9534	2384.582361	-43746.81958	20200305	45	kny	31.424	130.88	32523.31208	-3937.392708	33352.49993	20200305
5	bdv	49.08	14.015	20408.24278	1476.498472	44384.11257	20200305	46	kou	5.21	307.269	26566.90834	-8649.159903	6534.03419	20200305
6	bel	51.836	20.789	18910.50938	2155.445069	46753.62417	20200305	47	lrm	-22.222	114.101	30377.57938	113.0718056	-43262.77563	20200305
7	bfo	48.331	8.325	21000.85431	971.8170139	43518.68674	20200305	48	lyc	64.612	18.748	12954.21903	1788.108194	50824.92569	20200305
8	bmt	40.3	116.2	27901.35056	-4109.268472	47580.71354	20200305	49	mab	50.298	5.683	20026.52454	676.6008535	44643.7574	20200305
9	box	58.07	38.23	15149.76771	3423.754653	50605.48924	20200305	50	maw	-67.6	62.88	6637.389861	-17331.47576	-45610.43313	20200305
10	brd	49.87	260.026	15215.71021	1349.588194	54525.18188	20200305	51	mcq	-54.5	158.95	10702.30986	6865.926042	-62729.04792	20200305
11	brw	71.32	203.38	8896.940417	2040.051944	56567.42097	20200305	52	mea	54.616	246.653	13676.0725	3502.193194	55141.94083	20200305
12	bsl	30.35	270.364	23897.89611	-534.3659028	40619.165	20200305	53	mmb	43.91	144.189	25860.92479	-4160.602986	42601.24806	20200305
13	cbb	69.123	254.969	5052.641181	515.9493056	58112.67063	20200305	54	ngk	52.072	12.675	18870.10889	1331.096806	45797.97604	20200305
14	cki	-12.187	96.834	34897.57944	-1267.207778	-32411.88188	20200305	55	nur	60.508	24.655	14746.53667	2287.914931	50328.62708	20200305
15	clf	48.025	2.26	21268.24681	374.1634028	43038.32201	20200305	56	nvs	54.85	83.23	15977.18264	2267.85125	57794.77472	20200305
16	cmo	64.871	212.139	12071.0441	3662.327361	55060.79042	20200305	57	ott	45.403	284.448	18006.06139	-4293.210347	50757.78646	20200305
17	cnb	-35.314	149.363	23121.84965	5192.365069	-52948.43965	20200305	58	pag	42.515	24.177	23724.57785	2052.341181	41095.60694	20200305
18	cpl	17.293	78.92	39453.13201	-510.5802778	17435.07875	20200305	59	pet	52.971	158.248	21521.23347	-2453.807986	47410.99722	20200305
19	csy	-66.28	110.53	-1183.919167	-8905.680139	-63455.59493	20200305	60	pil	-31.667	296.119	18525.13889	-1971.772847	-12926.00313	20200305
20	cta	-20.09	146.264	31415.04941	4032.899791	-37523.00592	20200305	61	pst	-51.704	302.107	17998.51828	816.7563025	-21589.41492	20200305
21	dou	50.1	4.599	20166.69694	564.5751389	44377.19028	20200305	62	res	74.69	265.105	2821.225278	-966.5449306	57412.04722	20200305
22	dur	41.65	14.467	24664.39583	1661.169444	39635.57229	20200305	63	sba	-77.85	166.762	-10322.08271	5515.313542	-65094.66458	20200305
23	ebr	40.957	0.333	25322.75201	348.5455556	37632.16313	20200305	64	sbl	43.932	299.991	20099.86778	-6159.527222	45830.59819	20200305
24	frd	38.201	282.63	21211.1253	-3948.038707	45969.93919	20200305	65	sfs	36.667	354.055	27692.98333	-437.525625	33061.71813	20200305
25	frn	37.091	240.281	22610.76882	5106.934306	41905.74014	20200305	66	she	-15.961	354.253	16010.89917	-3784.684444	-25849.75875	20200305
26	fur	48.165	11.277	20993.37243	1266.938681	43689.14313	20200305	67	sit	57.058	224.675	15003.98639	5020.095972	52959.09139	20200305
27	gan	-0.695	73.154	38064.10701	-2720.955278	-12852.37549	20200305	68	sjg	18.111	293.85	26371.23667	-6125.861667	24778.29694	20200305
28	gck	44.63	20.77	22705.50861	1968.7925	42322.95653	20200305	69	spg	60.542	29.716	14451.77243	2766.171111	50554.4159	20200305
29	gng	-31.356	115.715	24154.41201	-695.7534028	-52657.5475	20200305	70	spt	39.547	355.651	26157.41243	-212.2654861	35974.31007	20200305
30	gui	28.321	343.559	27788.94125	-3297.265486	22532.55771	20200305	71	tam	22.792	5.53	33853.35556	317.1153472	17125.37632	20200305
31	had	50.995	355.516	19815.59375	-487.1833333	44458.94479	20200305	72	tdc	-37.067	347.684	9158.353472	-3520.939514	-22389.23111	20200305
32	hbk	-25.883	27.707	12484.80071	-4183.221111	-24963.03222	20200305	73	thl	77.47	290.77	3048.201319	-2836.9075	56138.82771	20200305
33	her	-34.425	19.225	9607.833819	-4713.809861	-22995.42292	20200305	74	thy	46.9	17.893	21518.14722	1798.217431	43480.7241	20200305
34	hlp	54.603	18.811	17482.39139	1693.542639	47405.90799	20200305	75	tsu	-19.202	17.584	14031.38007	-2157.920833	-25488.01035	20200305
35	hrb	47.875	18.19	20998.77708	1814.178403	44071.71535	20200305	76	tuc	32.174	249.266	23874.2234	3757.009861	40291.74611	20200305
36	hyb	17.42	78.55	39586.70764	-409.4116667	18254.32278	20200305	77	ups	59.903	17.353	15093.9141	1687.224931	49301.94847	20200305
37	iqa	63.756	291.49	8624.755702	-3943.983658	56107.03804	20200305	78	vic	48.517	236.583	18091.75582	5186.817181	49871.91367	20200305
38	irt	52.17	104.45	18339.39819	-1321.375208	57631.08368	20200305	79	vna	-70.683	351.718	18066.2466	-4484.883403	-33255.14722	20200305
39	izn	40.5	29.72	25075.98528	2459.532708	40544.37868	20200305	80	vss	-22.4	316.35	16425.94375	-6916.265278	-14993.05438	20200305
40	jco	70.356	211.201	8698.91	2596.038472	56590.54382	20200305	81	wic	47.928	15.862	21013.83049	1646.833889	43916.92826	20200305
41	kak	36.232	140.186	29794.62132	-4036.528194	35869.73299	20200305	82	wng	53.725	9.053	18186.19222	1002.707153	46352.84486	20200305

1 Results

The 24 Gaussian coefficients I have calculated are in Table 2

Tab 2. Gauss Coefficients my obtained (using quasi-Schmidt normalization)

Coefficent	Degree(n)	Order(m)	Value	Coefficent	Degree(n)	Order(m)	Value
g	1	0	-29017.523	h	3	1	-42.65915408
g	1	1	-1858.68841	h	3	2	600.217349
h	1	1	4903.10927	h	3	3	-633.5583365
g	2	0	-2497.135416	g	4	0	1132.882537
g	2	1	2617.981296	g	4	1	1296.172272
g	2	2	2178.890222	g	4	2	-2.933163263
h	2	1	-3201.763686	g	4	3	-357.3671095
h	2	2	-923.4214529	g	4	4	120.6542625
g	3	0	805.1006385	h	4	1	486.9660327
g	3	1	-2166.619627	h	4	2	-230.1865231
g	3	2	1281.757376	h	4	3	195.544086
g	3	3	90.1221627	h	4	4	-207.4272451

In order to evaluate the fitting effect of the model on the data, the prediction data on the original observation point were obtained by using $\mathbf{E} = \mathbf{Am}$, and the error between the observation value and the prediction value was calculated, as shown in Figure 2, 3:

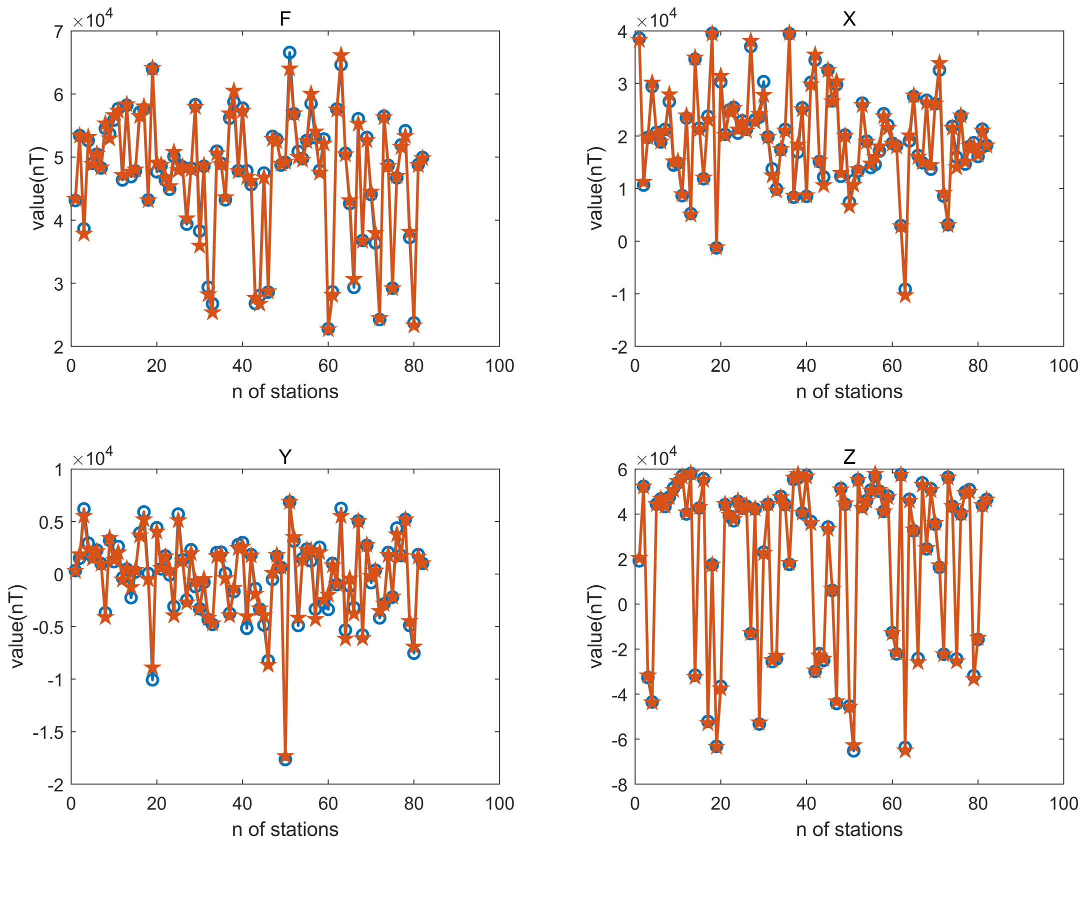

Fig 2. Maps of observation value and prediction value

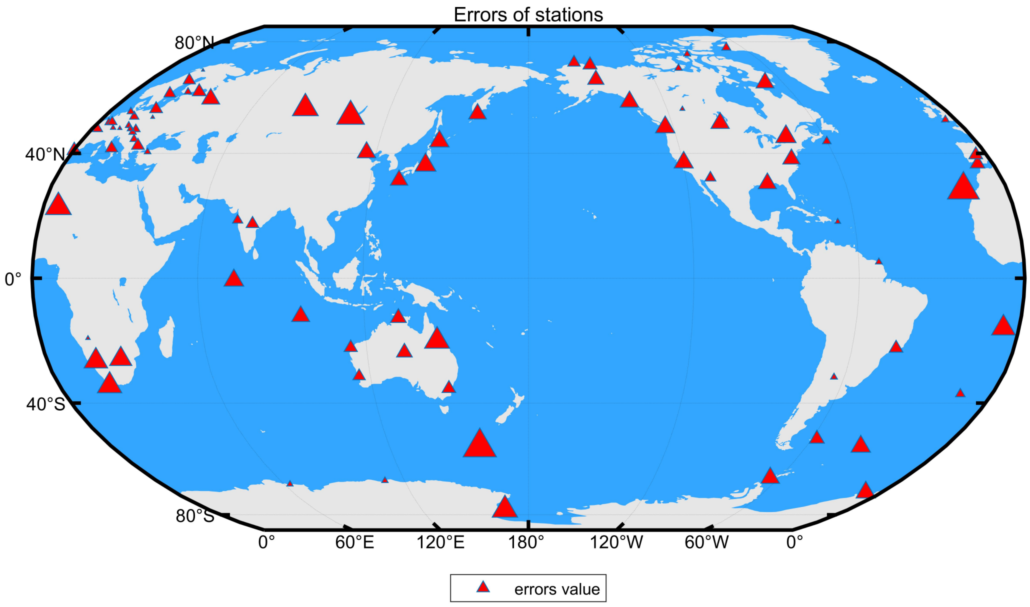

Fig 3. Maps of errors at each observational stations

2 Global model from inverse Gauss Coefficient

The inverse Gauss coefficient can be used to calculate the global magnetic field distribution, which has been shown in Figure 4-11

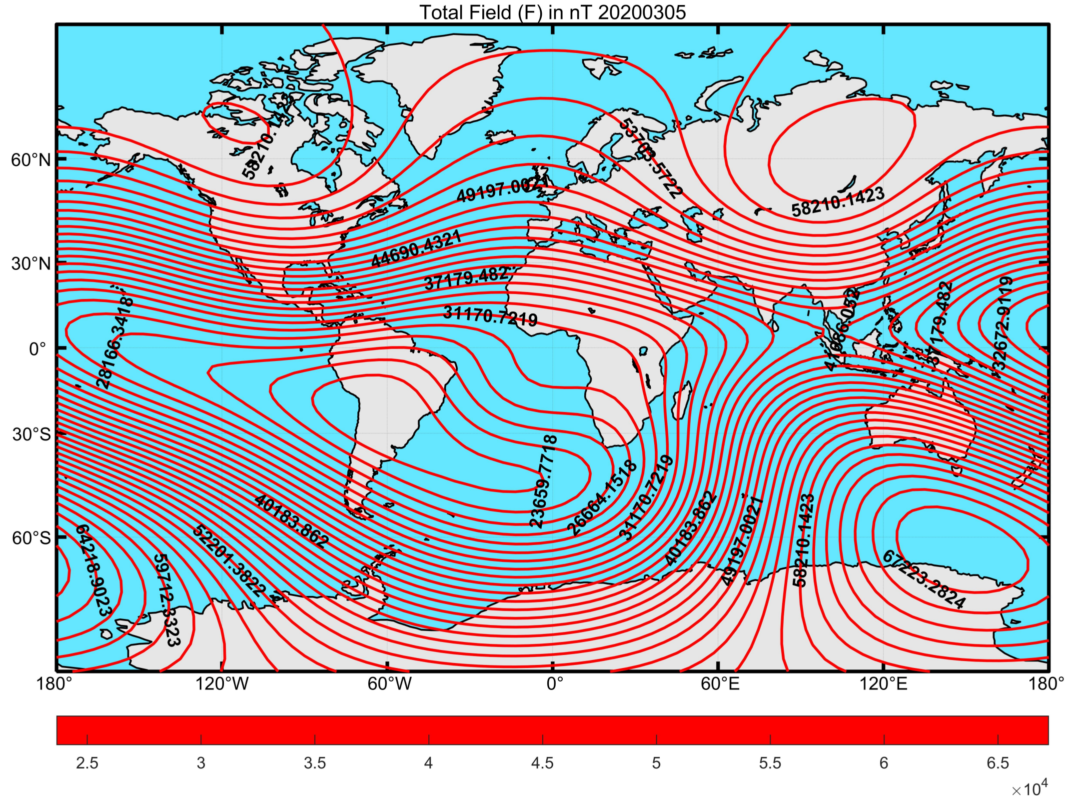

Fig 4. Contour-maps of the total field intensity F

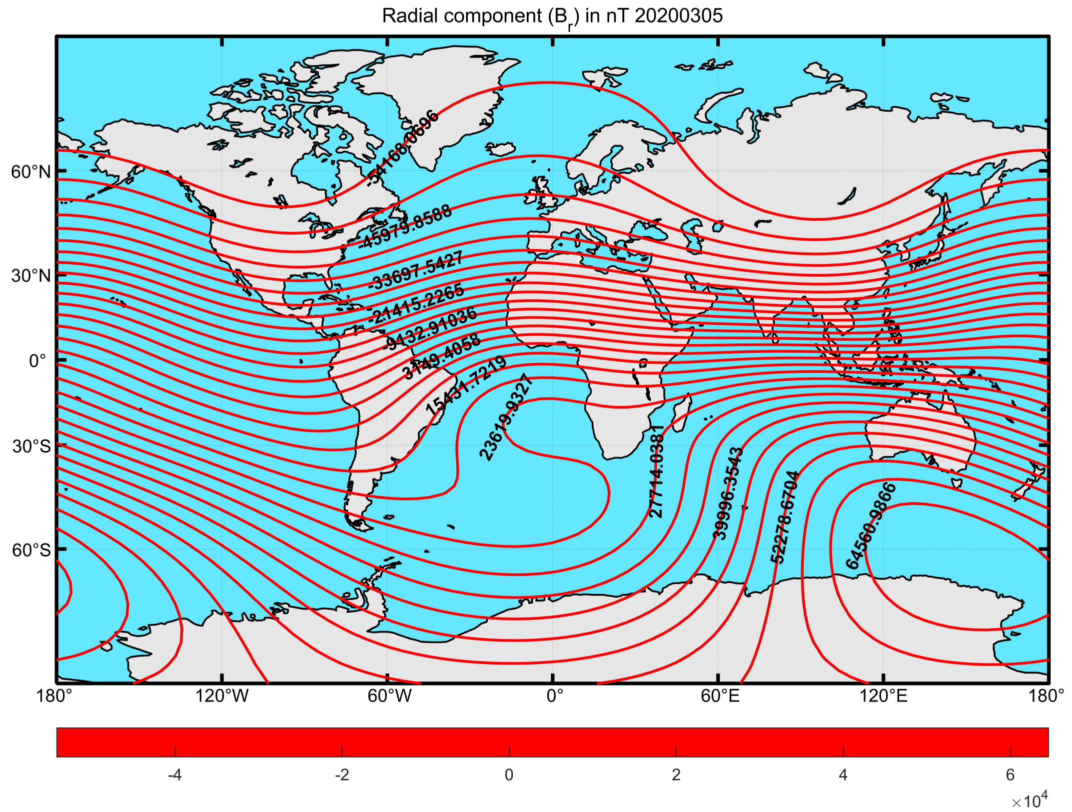

Fig 5. Contour-maps of the radial component Br

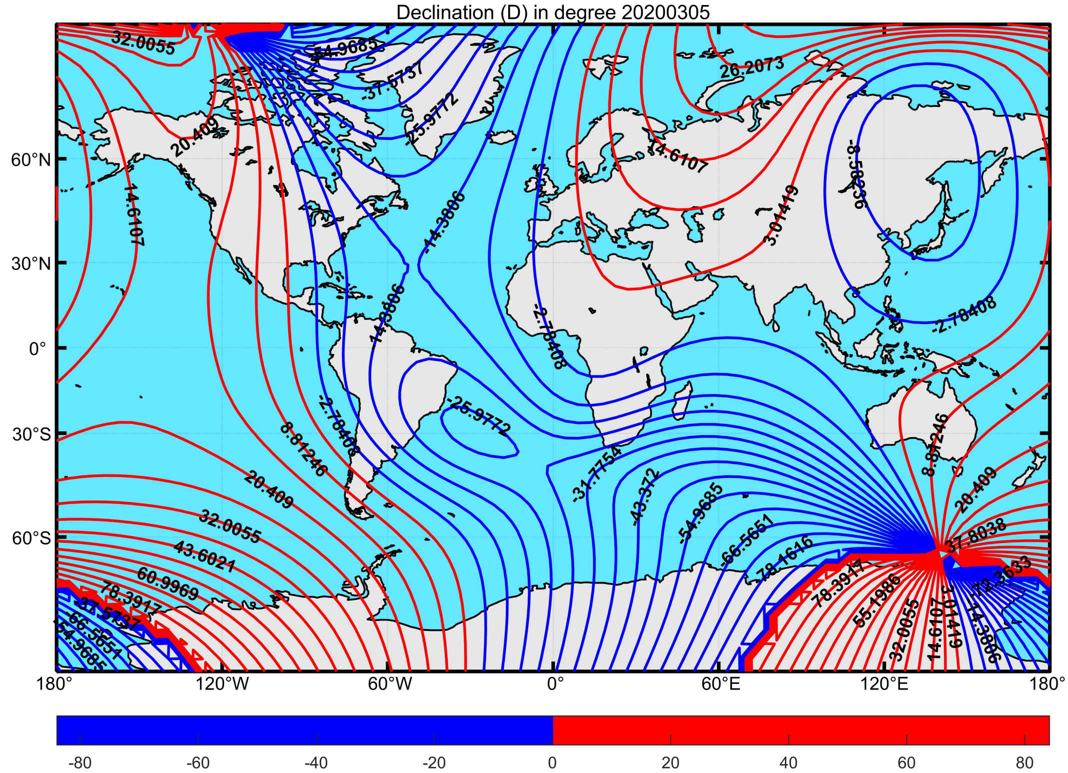

Fig 6. Contour-maps of the Declination D

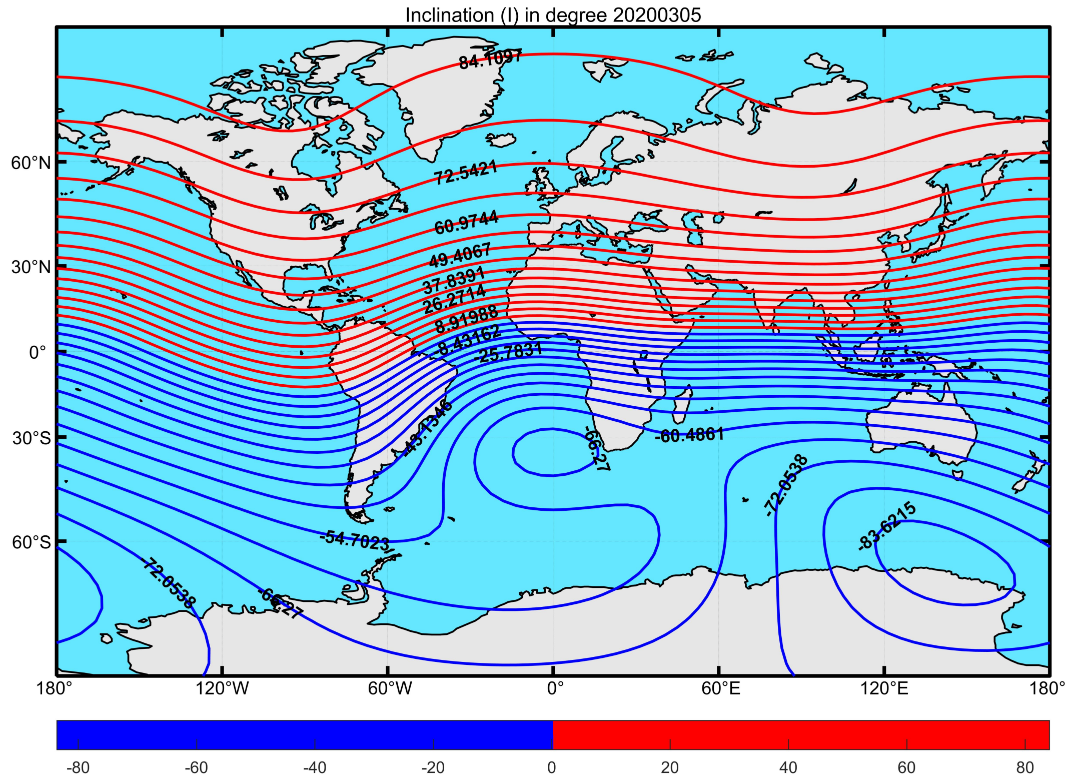

Fig 7. Contour-maps of the Inclination I

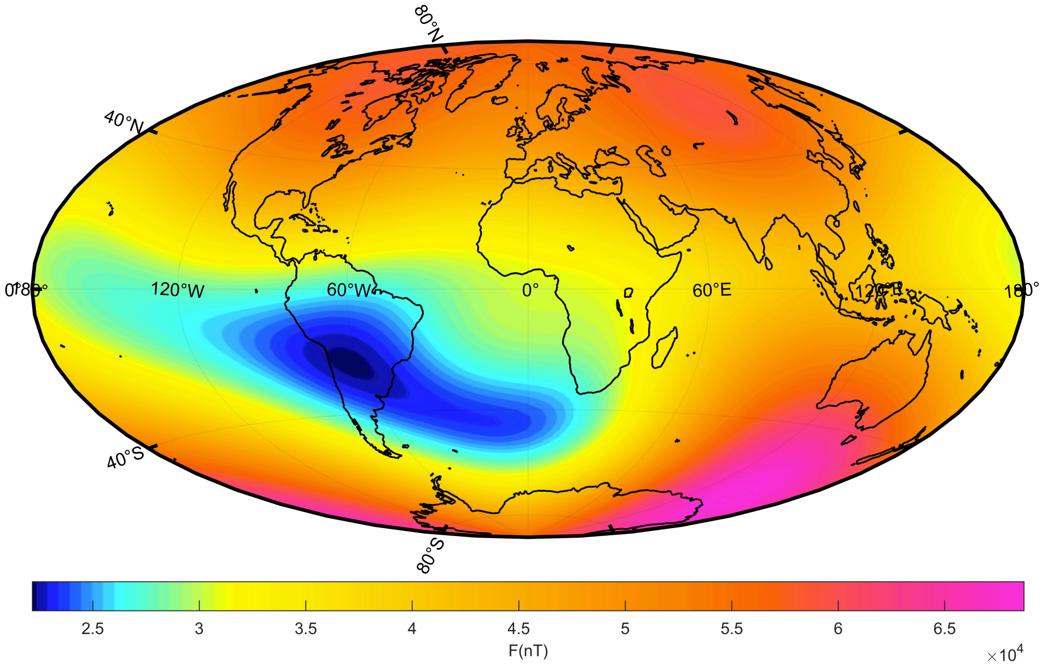

Fig 8. Contourf-maps of the total field intensity F

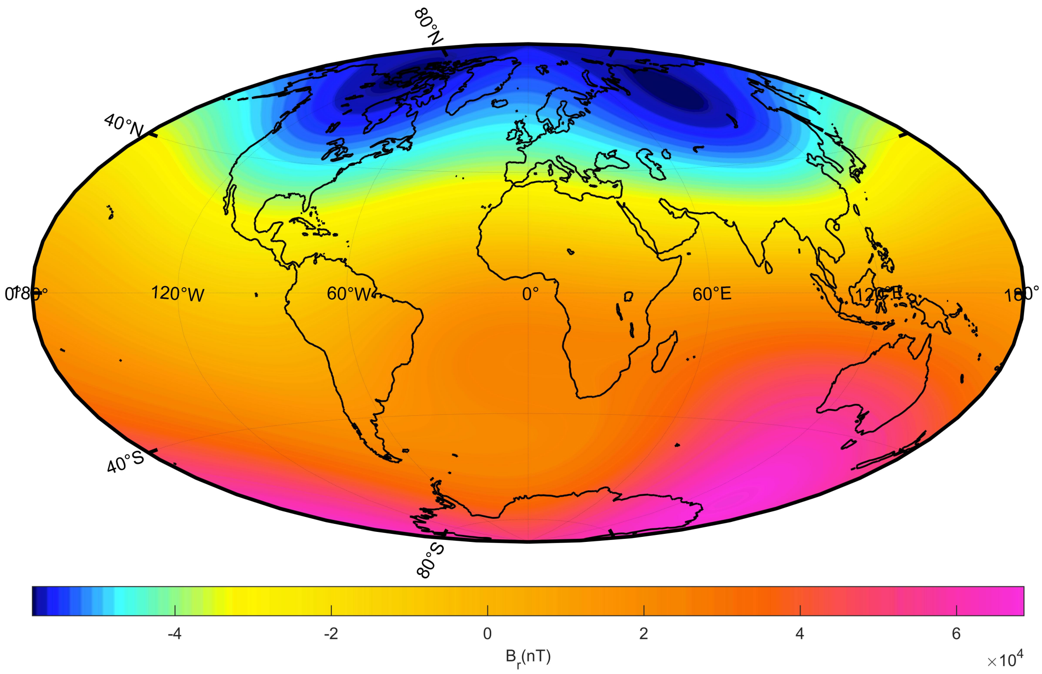

Fig 9. Contourf-maps of the radial component Br

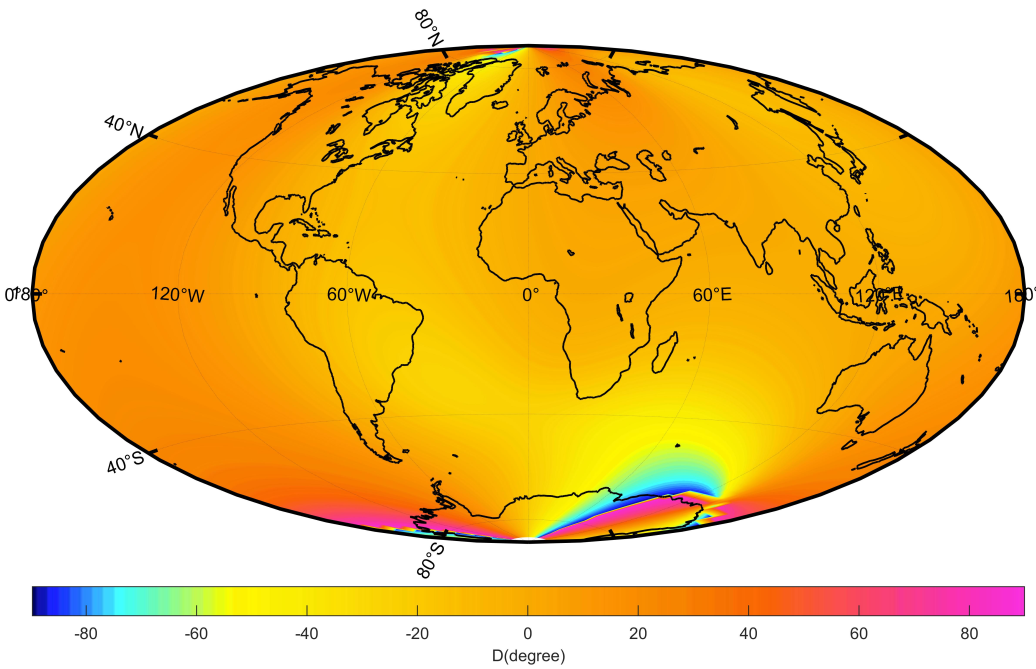

Fig 10. Contourf-maps of the Declination D

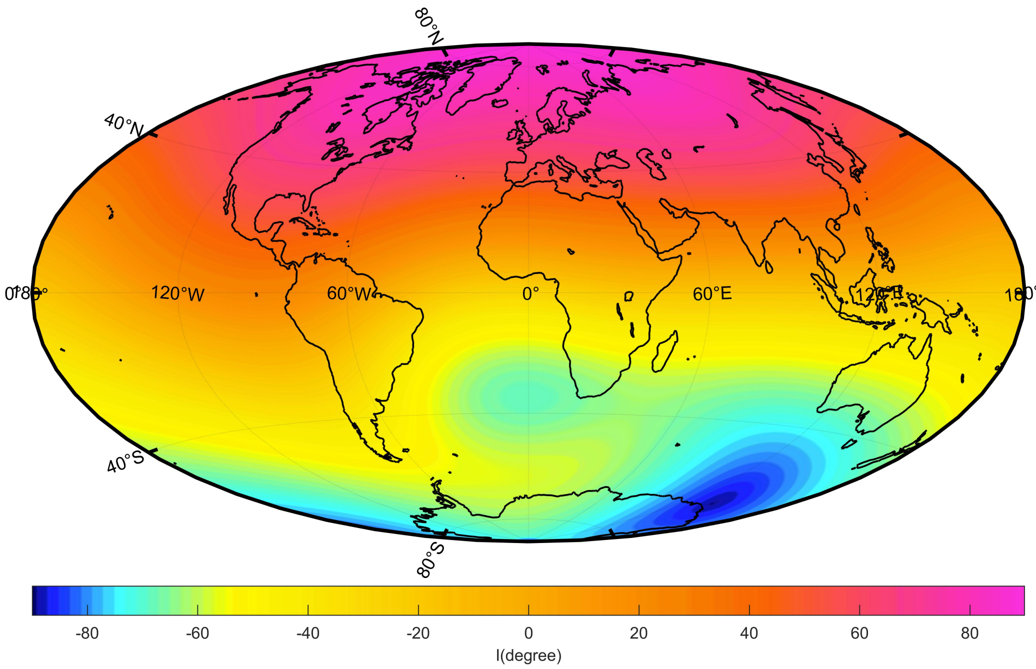

Fig 11. Contourf-maps of the Inclination I

It is obvious that the South Atlantic magnetic anomaly is consistent with the known characteristics of the geomagnetic field, indicating that our model can reflect the characteristics of the geomagnetic field to a certain extent.

3 Comparison with IGRF-13

Compute the spectrum in SH degree by:

$$S(n) = (n+1)\sum_{m=0}^{n}(g_n^m)^2 + (h_n^m)^2 \tag{6}$$

and compare them with the results of IGRF-13 (Figure 12) shown that the inversed Gauss coefficients are in good agreement with IGRF-13 model. The characteristics of the main earth's magnetic field are almost the same, except for a small deviation when the degree is high.

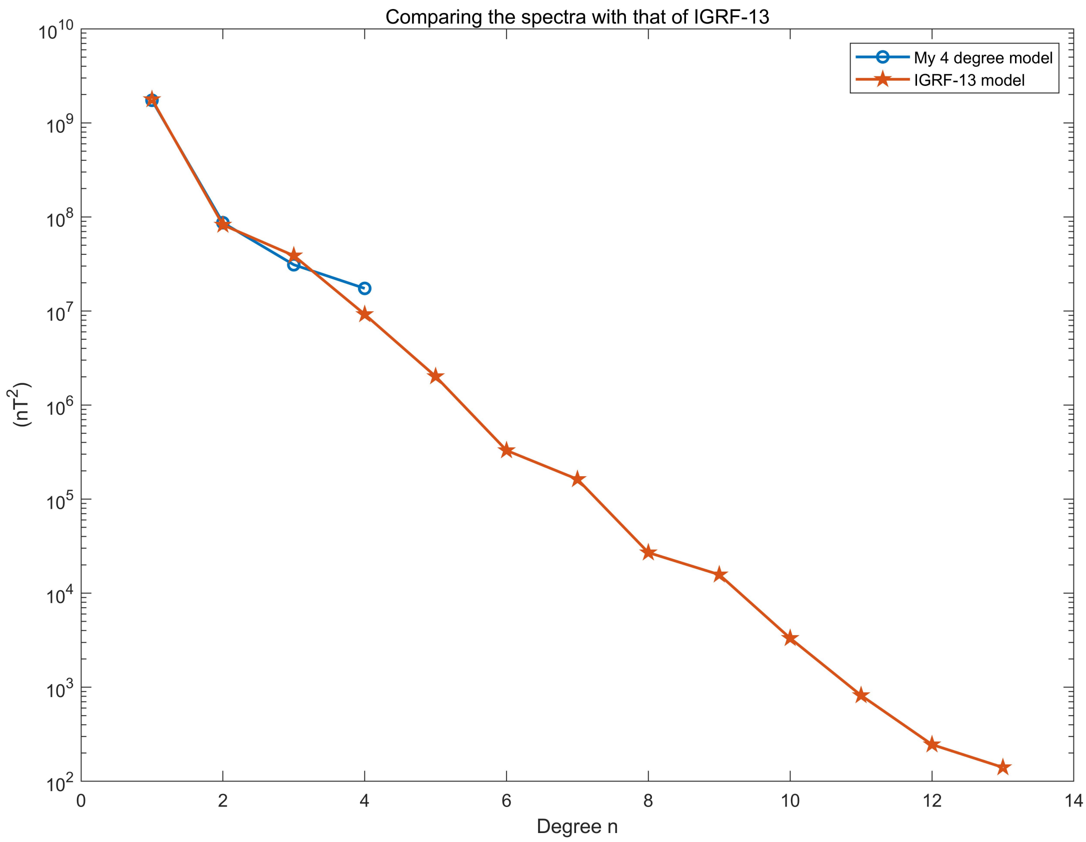

Fig 12. A plot comparing the spectra of my model with that of IGRF-13

4 Discussion

Through the inversion of the observed data, I got 24 Gauss coefficients, and used them to establish the global magnetic field model, draw the magnetic field distribution on the surface of earth. Compared with the IGRF-13 model, it has good consistency, but there are still subtle differences. The reason is that when we sift through the data, the distribution of observation stations is not well-distributed enough, and we can not achieve uniform distribution on a global scale. Therefore, the inversed model is greatly affected by the local data, even if we increase the degree of the spherical harmonic coefficient will not help, there will be even greater difference. If our model is to be more accurate, it will need to include satellite data that can orbit the Earth around, which will also take into account the effects of external fields on the geomagnetic field, making the model more accurate.

5 Reference

[1] 聂琳娟, 许智铭. 利用SWARM星群磁测数据反演地球主磁场模型WHU-MM01[J]. 测绘地理信息, 2020, 45(05): 16–19.

[2] 徐文耀, 区加明, 杜爱民. 地磁场全球建模和局域建模[J]. 地球物理学进展, 地球物理学进展, 2011, 26(2): 398–415.

[3] Monika Korte, Catherine Constable. Continuous global geomagnetic field models for the past 3000 years[J]. Physics of the Earth and Planetary Interiors, 2003, 140(1): 73–89.

[4] N. W. Peddie. USGS model coefficients for continental U.S. and Hawaii (1985)[J]. Planetary and Space Science, 1992, 40(4): 561.

[5] An Homage to Gauss and His Model of the Earth’s Magnetic Field[J]. CMS Notes, .

[6] Davis J. Mathematical Modeling of Earth’s Magnetic Field[J]. .

[7] 白春华, 徐文耀, 康国发. 地球主磁场模型[J]. 地球物理学进展, 2008(4): 1045–1057.

[8] 冯春. Matlab实现IGRF国际地磁参考场模型的计算[J]. 内蒙古石油化工, 2014, 40(12): 43–46.

[9] 安振昌. 地磁场区域模型与全球模型的比较和讨论[J]. 物探与化探, 1991(04): 248–254.

[10] 刘元元, 王仕成, 张金生, 等. 最新国际地磁参考场模型IGRF11研究[J]. 地震学报, 2013, 35(1): 125-131+133-134+138.

[11] International Geomagnetic Reference Field (IGRF-13)[EB/OL]. /2022-05-28. https://wdc.kugi.kyoto-u.ac.jp/igrf/index.html.

[12] Alken P, Thébault E, Beggan C D, 等. International Geomagnetic Reference Field: the thirteenth generation[J]. Earth, Planets and Space, 2021, 73(1): 49.

[13] Finlay C C, Kloss C, Olsen N, 等. The CHAOS-7 geomagnetic field model and observed changes in the South Atlantic Anomaly[J]. Earth, Planets and Space, 2020, 72(1): 156.